

## 안정성층류에서 선택취수의 수치해석

### Numerical Simulation of Selective Withdrawal in Stably Stratified Flows

백 중 철\*

Paik, Joongcheol

#### Abstract

A three-dimensional thermal hydrodynamic model is developed for carrying out unsteady simulation of the selective withdrawal of the stably stratified flow in a geometrically complex, natural reservoir. The governing equations are discretized on a non-staggered grid using a second-order accurate, finite-volume scheme. The numerical model is validated by applying it to simulate three-dimensional, turbulent, stratified, shear-layer flow case. The numerical predictions appear to capture reasonably well the general shape of velocity and temperature profiles observed in the laboratory experiments, while significant overestimation of the magnitude of velocity profiles is observed in the application to the flow in a natural reservoir. The physics of selective withdrawal as emerge from the numerical simulations are also discussed.

*keywords* : three-dimensional, thermal hydrodynamic model, selective withdrawal, stratified flow, shear flow

#### 요 지

3차원 열동수역학 모형을 개발하여 지형학적으로 복잡한 자연 저수지에서 안정한 성층류의 선택 취수를 부정류 모의하였다. 지배방정식은 2차 정확도의 유한체적법을 이용하여 해석하였다. 개발된 수치모형을 3차원 난류, 성층화된 전단층흐름에 적용하여 검정을 하였다. 수치해석결과는 실험실에서 관측된 선택취수시의 속도 및 온도분포의 일반적인 형상을 양호하게 예측하는 것으로 나타났으나, 자연 저수지에서의 흐름에 대한 적용시에는 속도의 크기를 과대모의 하는 것으로 나타났다. 수치모의에서 구해진 선택취수의 물리적 특성을 논하였다.

**핵심용어** : 3차원, 열동수역학 모형, 선택취수, 성층류, 전단류

#### 1. Introduction

A line or point sink located at the bottom of an initially stagnant body of water will draw from the entire water column when temperature stratification is very weak. Under the presence of significant thermal stratification, however, the same source

will draw water selectively from a certain portion of the water column. This phenomenon is known in the literature as selective withdrawal and its physics depend critically on the relative magnitudes of the inertial, viscous, and gravity forces (Debler, 1959). Selective withdrawal is exploited in reservoirs to facilitate downstream water usage and in water

\* 조지아공대 토목환경공학과, 연구공학자(연구교수)  
Research Engineer, School of Civil and Environmental Engineering, Georgia Institute of Technology, Atlanta, Georgia 30332-0355, USA. (e-mail: joongcheol.paik@ce.gatech.edu)

treatment plants to control water quality. Because of its fundamental and practical significance, the phenomenon has been and continues to be the subject of considerable experimental (Imberger, 1972; Pao et al., 1974; Ivey and Blake, 1985), theoretical and computational work (Pao and Kao, 1974; McGuirk and Islam, 1987; Wood, 2001; Forbes and Hocking, 2003).

Pao and Kao (1974) were the first to provide a comprehensive explanation of the physics of selective withdrawal for the two-dimensional case. They reported numerical simulations and experiments, which showed that a steady-state withdrawal layer is established via a transient state characterized by trains of internal shear waves propagating outward from the sink against the induced flow velocity—see Pao and Kao (1974), Pao et al. (1974), and Imberger (1980). As pointed out by Fischer et al. (1979), however, the axisymmetric (point sink) rather than the two-dimensional problem studied by Pao and Kao (1974) is often more relevant in engineering applications. These applications include condenser cooling water intakes in shallow coastal areas and water treatment intakes in lakes (Rodi, 1987). In these applications water is drawn from one or more cylindrical intake structures, through a circular or annular opening, located at the bottom of a shallow body of water.

Because of the complexity of the flow during the transient stage of withdrawal, in essence, all previous experimental work have focused on characterizing the final steady or quasi-steady state flow and developing empirical design equations. Thus, very little is known about the rich dynamics of these transients and the manner in which internal shear waves interact with the flow to set up the selective withdrawal layer. Computational fluid dynamics could in principle provide useful insights into these phenomena but the dominant role of the internal shear waves in such flows makes their numerical simulation a rather formidable undertaking. Consider, for example, an intake structure located at the bottom of a lake whose size is essentially infinite when compared to the size of the intake. Upon the start of withdrawal and in the presence of

stratification in the water column, internal waves will begin propagating away from the sink. Depending on the relative importance of the inertial, viscous, and buoyancy forces, these waves will either propagate to infinity and decay (viscous forces and buoyancy dominate) or be balanced by the incoming flow (inertial forces and buoyancy dominate) to form standing wave patterns (Imberger 1980). In either case the radial distance from the sink where the transients decay may be very long. From the numerical standpoint, these complex transients pose a unique challenge. Simulating the flow in the entire lake is not practical if one is interested in the details of the flow in the vicinity of the intake. Instead, truncating the computational domain at some radial distance from the sink is the only practical alternative. The flow conditions at this inflow boundary, however, are not known a priori because the flow entering the computational domain is continuously being modified by the transient shear waves—to be precise the only quantity known at this boundary is the volume flow rate drawn by the sink. Therefore, the situation in this case is quite different from what this study encountered in most fluid flow problems where eddies exit through an outflow boundary. In this case the challenge stems from the need to specify a set of dynamic, non-reflective inflow boundary conditions, which allow transients waves to cross and propagate to infinity.

In spite of growing recent interest in the numerical simulation of various stratified flow problems, only a handful of researchers have attempted to simulate numerically selective withdrawal. Pao and Kao (1974) used a first-order accurate, vorticity-stream function formulation to simulate selective withdrawal from a line sink (2D case). They employed exponential coordinate stretching in the direction of the flow, which in essence resulted in rapidly expanding grid spacing away from the sink. The very coarse mesh in the far-field region in conjunction with the first-order accuracy of their method presumably resulted in the damping of the transient waves, thus, allowing the sink flow to approach a steady state. McGuirk and Islam (1987) simulated 2D selective withdrawal both in a closed container and in a

semi-infinite domain using a pressure-based SIMPLE-type method. Note that the closed-container case can represent the actual flow situation only for a finite time until the internal waves reach the container wall and reflect into the domain to affect the flow. For the semi-infinite case, McGuirk and Islam (1987) specified uniform flow at the far-field boundary and could, thus, carry out their simulations only for times shorter than the time it took for the fastest traveling shear waves to reach the far field boundary. Beyond that time, wave reflections at the far-field boundary would ultimately contaminate the flowfield near the sink and render the simulation ill-posed.

This work seeks to develop a second-order accurate primitive-variable numerical method capable of simulating selective withdrawal in thermally stratified domains. This study also seeks to demonstrate that the method can be used to obtain steady-state solutions that are independent of the domain size. The unsteady, Boussinesq continuity, Navier-Stokes and temperature transport equations for an incompressible, Newtonian fluid are solved numerically. The continuity and Navier-Stokes equations are discretized on a non-staggered grid using second-order accurate finite-difference formulas. The discrete equations are integrated in time using a dual-time-stepping artificial compressibility algorithm. At the far-field boundary, the pressure, velocity components, and temperature are obtained by solving a reduced version of the Boussinesq equations. These equations are derived by extending into incompressible flows and adapting for stratified flow the characteristic-based approach developed by Thompson (1987) and Poinot and Lele (1991) for the compressible Navier-Stokes equations.

The paper is organized as follows. First the physical problem is described and the governing equations are formulated in general, curvilinear coordinates. Subsequently the numerical method is presented briefly. This is followed by numerical tests of the developed model. And simulation results for the selective withdrawal of the stably stratified flow in a geometrically complex reservoir are presented and the physics of selective withdrawal is discussed.

Finally this paper concludes with a summary of the findings and discussion of future research directions.

## 2. Governing Equations

For a thermally-stratified flow the density changes in the fluid are caused by the temperature variations. The Boussinesq approximation is applicable when the temperature variation is small. The computational domain is assumed to be filled with incompressible fluid of a reference density  $\rho^*$  and viscosity  $\nu^*$  where the superscript \* denotes the dimensional variable. The free surface elevation is  $H^*$  and is assumed to remain flat and fixed at all times. The lake is thermally stratified with an initial step-like temperature profile. The epilimnion and hypolimnion temperatures are  $T_e^*$  and  $T_h^*$ , respectively, and the thermocline is located at depth  $h^*$ . The stratification is assumed to be stable, that is  $T_h^* < T_e^*$ . The intake begins to draw impulsively at  $t=0$  from an annular opening at its top at constant flow rate  $q^*$ . Lengths are non-dimensionalized with  $H^*$  and velocities with the intake bulk velocity  $V^*$ . A non-dimensional temperature variable  $T$  is defined as follows:

$$T = \frac{T^* - T_h^*}{T_e^* - T_h^*} \quad (1)$$

where  $T^*$  is the dimensional temperature. Density variations are assumed to be caused by temperature variations, which are sufficiently small for the Boussinesq approximation to be applicable. Under these assumptions the flow is governed by the so-called Boussinesq equations, the incompressible continuity equation, the Navier-Stokes equations with buoyancy terms and the transport equation for the stratification-inducing scalar (the temperature in this case) –see Kundu (1990) for a detailed derivation of the Boussinesq equations. In this study, the governing equations are non-dimensionalized by reference length  $H^*$ , reference velocity  $V^*$ , reference temperature  $T^*$  and reference molecular viscosity of fluid  $\nu^*$ .

The governing equations for the mean flow are the

three-dimensional, unsteady, incompressible, Reynolds-averaged Navier-Stokes (RANS) equations. By invoking the Boussinesq hypothesis to express the Reynolds stresses in terms of the mean rate of strain tensor, the governing equations for the mean flow can be written in strong-conservation form in general, curvilinear coordinates as follows,

$$\Gamma \frac{\partial Q}{\partial t} + J \frac{\partial}{\partial \xi^j} (F^j - F_v^j) = 0 \quad (2)$$

where

$$\Gamma = \text{diag}[0, 1, 1, 1] \quad (3)$$

$$Q = [P, u_1, u_2, u_3]^T \quad (4)$$

$$F_f^j = \frac{1}{J} [\beta U^j u_1 U^j + p \xi_{s1}^j, u_2 U^j + p \xi_{s2}^j, u_3 U^j + p \xi_{s3}^j - T / Fr^2]^T \quad (5)$$

$$F_v^j = \frac{1}{J} \left( \nu_t + \frac{1}{Re} \right) \left[ 0, g^{mj} \frac{\partial u_1}{\partial \xi^m}, g^{mj} \frac{\partial u_2}{\partial \xi^m}, g^{mj} \frac{\partial u_3}{\partial \xi^m} \right]^T \quad (6)$$

The governing equation for the temperature is

$$\frac{\partial T}{\partial t} + J \frac{\partial}{\partial \xi^m} \left[ \frac{1}{J} \left( UT - \left( \frac{1}{\sigma Re} + \frac{\nu_t}{\sigma_i} \right) g^{mj} \frac{\partial T}{\partial \xi^m} \right) \right] = 0 \quad (7)$$

In the equations above, the term  $P$  is a modified pressure  $P = p/\rho + 2k/3$  where  $P$  is the piezometric pressure and  $k$  is the turbulent kinetic energy  $u_i (i=1, 2, 3)$  are the Cartesian velocity components  $x_i$  are the Cartesian coordinates  $J$  is the Jacobian of the geometric transformation  $\xi_{x_j}^i$  are the metrics of the geometric transformation  $U^j$  are the contravariant velocity components  $U^j = u_i \xi_{x_j}^i$   $g^{ij}$  are the components of the contravariant metric tensor  $g^{ij} = \xi_{x_k}^i \xi_{x_k}^j$  and  $\nu_t$  is the turbulent viscosity. In the governing equations,  $Fr$  is the densimetric Froude number, which for the above introduced scaling is defined as follows:

$$Fr = \frac{V^*}{\sqrt{\beta g^* H^* (T_e^* - T_h^*)}} \quad (8)$$

where  $\beta$  is the coefficient of volumetric expansion of the fluid  $\sigma$  is the molecular Prandtl number  $\sigma_t$  is the turbulent Prandtl number  $g^*$  is the gravitational acceleration and  $Re$  is the Reynolds number:

$$Re = \frac{V^* H^*}{\nu^*} \quad (9)$$

A simple mixing-length eddy-viscosity model, modified to account for stratification effects on the structure of turbulence, is used to calculate the eddy viscosity  $\nu_t$ . The unmodified model is the standard mixing-length model according to which the eddy viscosity is calculated as:

$$\nu_t = l_m^2 S \quad (10)$$

where  $l_m$  is the mixing length defined as (Mason and Thomson, 1992):

$$\frac{1}{l_m} = \frac{1}{l_o} + \frac{1}{\kappa z} \quad (11)$$

The mixing length  $l_m$  is a function of the von Karman constant  $\kappa$ , the distance to the nearest wall  $z$  and  $l_o$  which is used to limit the rise in the mixing length. The variable  $S$  is the second invariant of the strain rate tensor defined as:

$$S = \frac{1}{2} \left( \frac{\partial u_i}{\partial x_j} + \frac{\partial u_j}{\partial x_i} \right)^2 \quad (12)$$

follows:

$$\nu_{to}, \quad \text{for } Ri < 0 \quad (13a)$$

$$\nu_{to} \sqrt{1 - Ri/Ri_c}, \quad \text{for } 0 \leq Ri \leq Ri_c \quad (13b)$$

$$0, \quad \text{for } Ri > Ri_c \quad (13c)$$

The limiting value of the Richardson number  $Ri$ , critical Richardson number  $Ri_c$ , beyond which turbulence can not be sustained ranges between 0.1 and 0.3 (Viollet 1980). The Richardson number is defined as:

$$Ri = \frac{1}{Fr^2} \frac{\partial T}{S^2} \quad (14)$$

To account for buoyancy effects, this study adopts the proposal of Mason (1989) who modified the above model to make the eddy viscosity as a function of the local Richardson number. The modified eddy viscosity  $\nu_t$  adjusted for buoyancy effects is calculated as

### 3. Numerical Methods

The governing equations formulated in generalized, curvilinear coordinates in strong conservation form are solved using a dual-time-stepping artificial compressibility (AC) iteration scheme. Due to space considerations, a brief description of the numerical methods is given in this paper (see Paik et al., 2005 for details). The AC forms of the governing equations are discretized using a second-order-accurate finite-volume method on a non-staggered computational grid. The convective terms are discretized using the QUICK scheme, and central differencing is employed for the pressure gradients, viscous fluxes and source terms in the temperature equation. The third-order artificial dissipation method of Sotiropoulos and Adballah (1992) is employed for pressure to eliminate odd-even decoupling of the pressure field. The physical time derivatives are discretized with three-point-backward, Euler-implicit temporal-integration scheme. The discrete equations are marched in time to advance the solution to the next time step by adopting the dual- (or pseudo-) time-stepping method which needs to be integrated in pseudo-time until the pseudo-time derivative is reduced to a prescribed small tolerance and the governing equations are satisfied at the advanced time level. The system of equations is integrated in

pseudo time using the pressure-based implicit preconditioner of Paik et al. (2005) enhanced with local-time-stepping and V-cycle multigrid acceleration.

A major difficulty in the numerical simulation of selective withdrawal from an axisymmetric source located at the center of a very large "lake" stems from the practical need to truncate the radial extent of the computational domain. At the far-field boundary, where flow enters into the domain, the velocity field is neither known a priori nor can it be assumed to be constant at all times as transient shear waves continue to modify the far-field flow over long periods of time. Steady or quasi-steady solutions can only be obtained if reflections are minimized by allowing the waves to exit the computational domain. Because the flow enters the computational domain through the far-field boundary, simple boundary conditions based on straightforward interpolation from the interior of the solution domain will fail as they will in general render the problem ill-posed. This paper will in fact show in a subsequent section that when extrapolation is used for all flow variables spurious, non-physical solutions are indeed obtained.

A set of boundary conditions is developed based on a truncated form of the governing equations obtained using the theory of characteristics for hyperbolic systems. This approach consists of the following three steps: 1) formulate the governing equations in dual-time, artificial compressibility form; 2) apply to the resulting pseudo-hyperbolic system of equations the characteristics-based approach proposed by Thomson (1990) to derive a set of evolution equations for the pressure and the velocity fields; 3) incorporate these equations into the iterative algorithm and use them to update the pressure, velocity and temperature fields at the far-field boundary. To develop this approach, this study treats only the continuity and Navier-Stokes equations as a coupled system. The coupling between these equations and the temperature equation, through the source term in the vertical momentum equation, will be ignored in the derivation without loss of generality since the temperature source term does not affect the structure of the characteristics (see Paik et al., 2005

for details). A truncated transport equation for the temperature field at the far-field boundary is obtained using a similar characteristics-inspired approach.

The boundaries such as the water surface, lake bottom, intake surfaces, and axis of symmetry all utilize fairly simple and robust boundary conditions. For all solid surfaces such as the intake and lake bottom, a no-slip condition is imposed for the velocity, a simple linear extrapolation for pressure, and a zero extrapolation for the temperature. A fixed surface elevation is used for the water surface for which the normal velocity vanishes and a zero order extrapolation is used for the parallel velocity. The pressure is linearly extrapolated from the surface.

#### 4. Model Validation

Here the RANS version of the numerical model is validated by applying it to simulate a three-dimensional, turbulent, stratified, shear-layer flow case for which experimental measurements were reported by Viollet (1980) who carried out both experiments and numerical simulations for a stably stratified shear flow consisting of a cool, fast-moving layer of fluid at the bottom and a warmer, slower-moving layer of fluid at the top as shown in Fig. 1. In this figure, subscripts t and b refer to top and bottom respectively. The governing equations are solved on a rectangular uniform grid consisting of 301, 25 and 69 nodes in the x-, y- and z-directions, respectively.

To calibrate and test the model, simulations are carried out for three cases: 1) Fr=0.9, Re=5000; 2)

Fr=1.6, Re=7500; and 3) Fr=5.0, Re=10000. All runs are made using a turbulent Prandtl number for temperature  $\sigma_t = 0.85$ . This is the ratio of the temperature diffusivity in water to the eddy diffusivity.

The calculated temperature and velocity profiles are compared with Viollet's (1980) measurements in Figs. 2 through 4. For all three cases it was found that the best fit with the experimental data is obtained for  $Ri_c$  within 0.25 to 0.30. For the Fr=0.9 case,  $Ri_c=0.1$  also gave similar results to those shown in Figure A.2 for  $Ri_c=0.25$ . A similar range of values for  $Ri_c$  was also reported by Viollet (1980) who used a two-equation k- model to simulate this flow and obtained results of comparable accuracy to those reported in this work—Viollet suggested a range for  $Ri_c$  between 0.1–0.3.

The calculated velocity profiles for all cases seems to agree well with experiment except for the profiles at  $x/h=5$  for which the maximum velocity is somewhat underestimated. However, at locations further downstream, the calculated velocity profiles are in very good agreement with the measurements. The exact reason for this discrepancy is not clear, but could be attributed to small discrepancies between the inlet conditions specified in the calculation and those in the experiment or erroneous reporting of data. It is obvious, however, that the effect of inconsistent inlet conditions in the calculation appears to diminish rapidly as the two layers begin to mix.

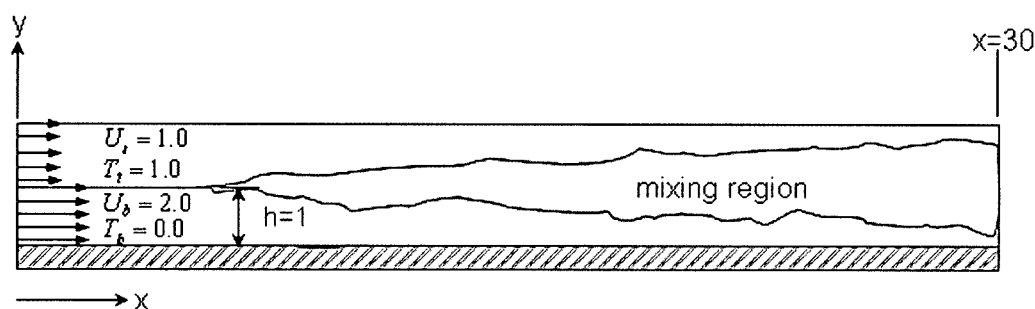


Fig. 1. Schematic of the stably stratified, turbulent plane-shear flow of Viollet's experiment

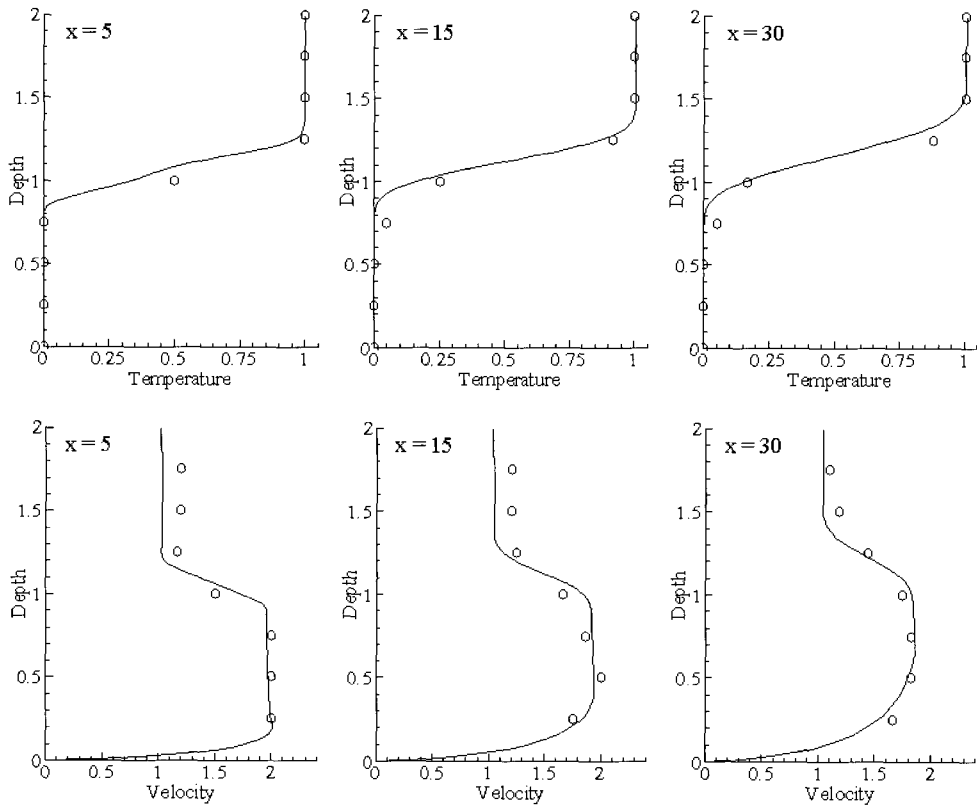


Fig. 2. Temperature and horizontal velocity profiles for  $Fr=0.9$ ,  $Re=5000$ , and  $Ri_c=0.25$  at three locations along the domain

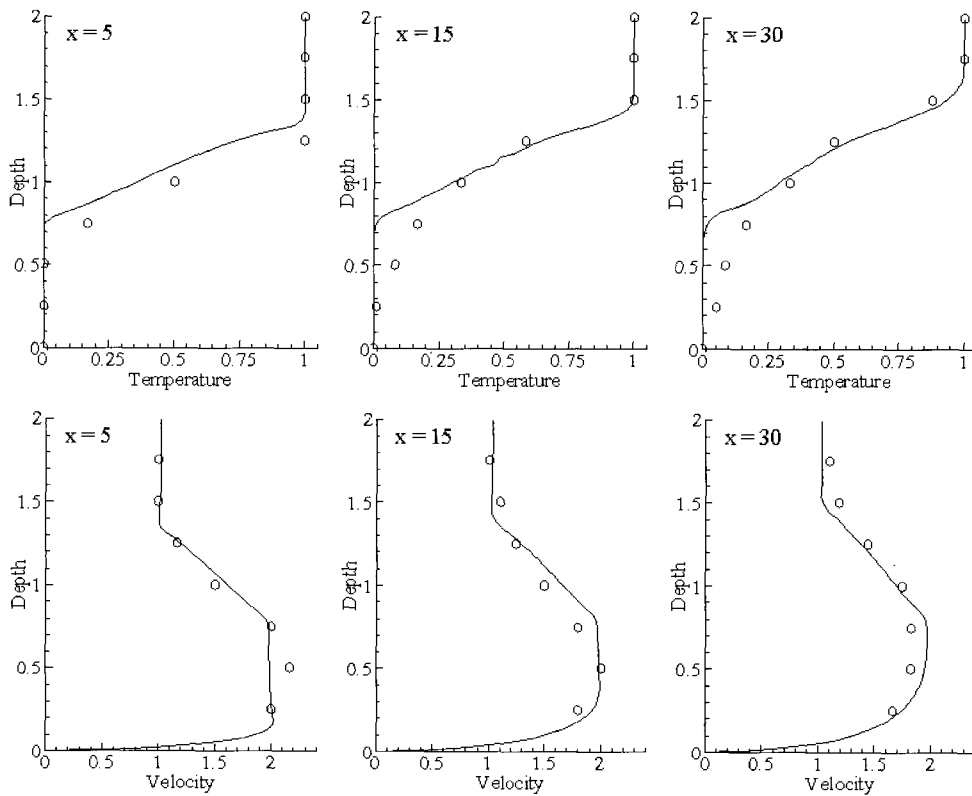


Fig. 3. Temperature and horizontal velocity profiles for  $Fr=1.6$ ,  $Re=7500$ , and  $Ri_c=0.25$  at three locations along the domain.

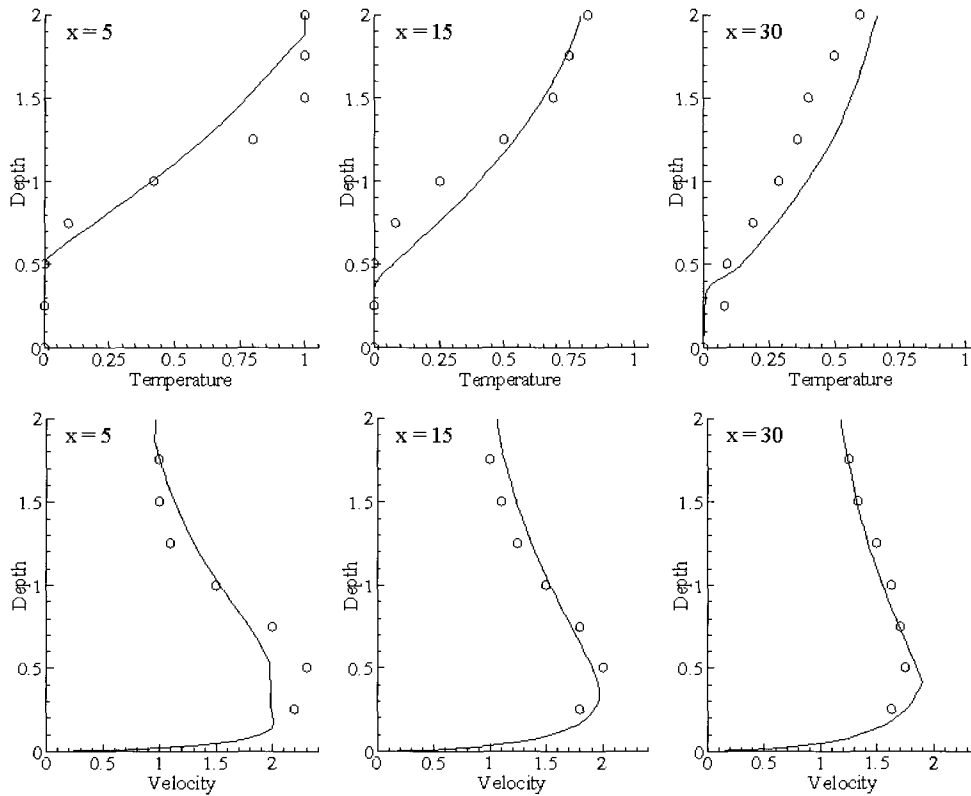


Fig. 4. Temperature and horizontal velocity profiles for  $Fr=5.0$ ,  $Re=10000$ , and  $Ri_c=0.3$  at three locations along the domain

The calculated temperature profiles for the  $Fr=0.9$  case are in better agreement with the experiments than those obtained for the two higher Froude numbers of 1.6 and 5.0. As the Froude number increases, the strength of the stratification weakens and turbulence dominates over buoyancy, which is evident by the relatively higher degree of mixing. The simulation resolves the temperature profile reasonably well near the surface but not as well near the mid-depth region and near the wall where the simulated profiles suggest both weaker and stronger mixing. A similar trend was also reported by other investigators who used Viollet's data for calibration of a depth-averaged model (Sladkevich et. al, 2000).

Despite the few noted differences between the simulations and experiments, the results are in reasonably good agreement with Viollet's experimental data. The results show that turbulent mixing of the temperature is enhanced as the Froude number increases and turbulence collapses for lower Froude numbers for which buoyancy effects dominate. The

simple algebraic mixing length model employed in this study appears to perform very well as the Froude number is decreased but its performance deteriorates somewhat at higher Froude numbers. Note that at low Froude numbers, the main function of the model is to suppress turbulence and apparently, the simple correction based on the Richardson number is effective in doing so. As the Froude number is increased and turbulence production is enhanced, the well known deficiencies of the mixing-length model such as the assumption of local equilibrium and absence of history and transport effects begin to dominate and lead to the observed deterioration of the model's performance.

## 5. Selective Withdrawal in a Reservoir

This study considers the withdrawal of cool bottom water from Lake Billy Chinook impounded by Round Butte dam on the Deschutes River, OR USA. The lake has a surface area of approximately 162 105 m<sup>2</sup> at normal high water surface elevation of 593



m above mean sea level, a maximum depth of more than 122 m near the dam, and a volume of approximately  $66\ 107\ \text{m}^3$ . At the mean annual flow ( $134\ \text{m}^3/\text{s}$ ), the residence time in Lake Billy Chinook is approximately 57 days. The peaking mode of operation and the inflow temperature characteristics, coupled with solar-heating of the surface water during summer, result in strong stratification of Lake Billy Chinook in the summer.

A domain decomposition method with embedded overset (Chimera) grids (Tang et al. 2003) is employed to simulate geometrical complexities of the powerhouse intakes. The computational domain for the bottom withdrawal case using the intake in the Forebay is discretized using two overset grids, as shown in Fig. 5. The grid is finely spaced in the vicinity of the intake to resolve the regions of intense velocity and temperature gradients. The total numbers of active grid nodes are approximately  $5.3 \times 10^5$ . In order to prescribe the velocity profiles exiting at the intake inlet in the bottom withdrawal case, this paper separately considered an additional grid structure and calculated flow fields. At the far-field boundary, where flow enters into the domain, the velocity field is neither known a priori nor can it be assumed to be constant at all times as transient shear waves continue to modify the far-field flow over long periods of time. Steady or quasi-steady solutions can only be obtained if reflections are minimized by allowing the waves to exit the computational domain. Because the flow enters the computational domain through the far-field boundary, simple boundary conditions based on straightforward interpolation from the interior of the solution domain will fail as they will in general render the problem ill-posed. Non-reflecting, characteristics-based boundary conditions are applied at the far-field boundary to allow vortical structures to exit the flow domain without spurious distortions (Paik et al. 2005).

The numerical simulation starts first for non-stratified flow case to access the effect of the thermal stratification on the selective withdrawal. In this case, large eddy was computed behind the intake tower and the water at all layers flows and

exits through the intake inlet, as shown in Fig. 6 which show snapshots of instantaneous stream traces colored by elevation in the entire computational domain. Unsteady solutions of the non-stratified flow case appear to actually converge to steady-state, which is more clearly visible in Fig. 7 showing the stream-traces near the intake. On the other hand, the selective withdrawal in a stratified environment is characterized by a layer of flow above or below which nearly stagnant flow or a large weak recirculation region exists as shown in Figs. 6(b) and 8. After a selective withdrawal layer has been established, the intake eddy continues to interact with upstream originating eddies. This interaction along with traveling shear waves along the thermocline results in an unsteady flow characterized by varying thickness of the withdrawal layer. Fig. 8 along with the animations show that the propagation of these multiple eddies forming just above the thermocline suppresses the flow streamlines and cause the intake to draw for the most part below and above the thermocline in the bottom withdrawal cases.

Measured and calculated time-averaged velocity and temperature profiles for the bottom withdrawal case are compared in Fig. 9, which also shows computed instantaneous profiles. This figure clearly shows the high unsteadiness of velocity field due to the thermal stratification even though the temperature profiles are relatively stable. The predictions of numerical simulation appear to capture the general shape of velocity and temperature profiles reasonably well, while significant overestimation of the magnitude of velocity profiles is observed. One possible explanation of this discrepancy could be the applied non-reflecting, far-field boundary conditions which depend only on the flow inside the computational domain. Quantitatively more accurate simulation expects to be obtained either by extending the computational domain further upstream to consider two river flows with different temperatures or by considering boundary condition computed by relatively simple numerical models.

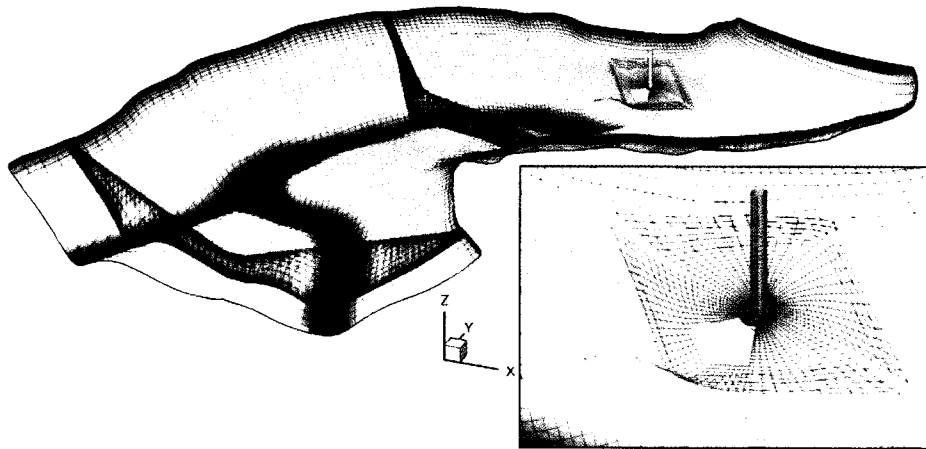


Fig. 5. Grid structures for the bottom withdrawal

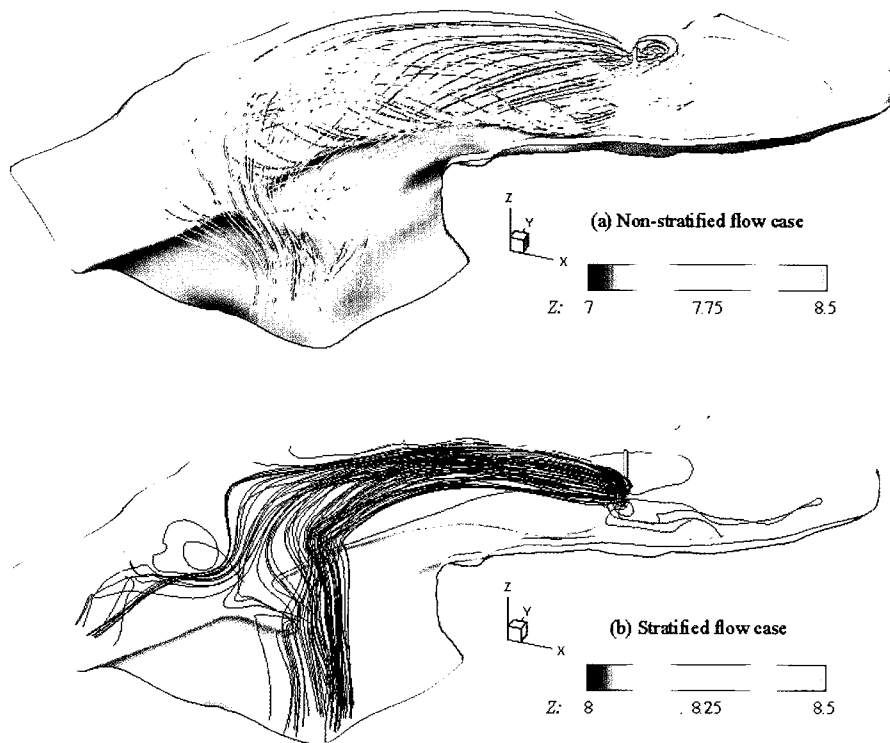


Fig. 6. Snapshots of instantaneous streamtraces colored by elevation in the entire computational domain.

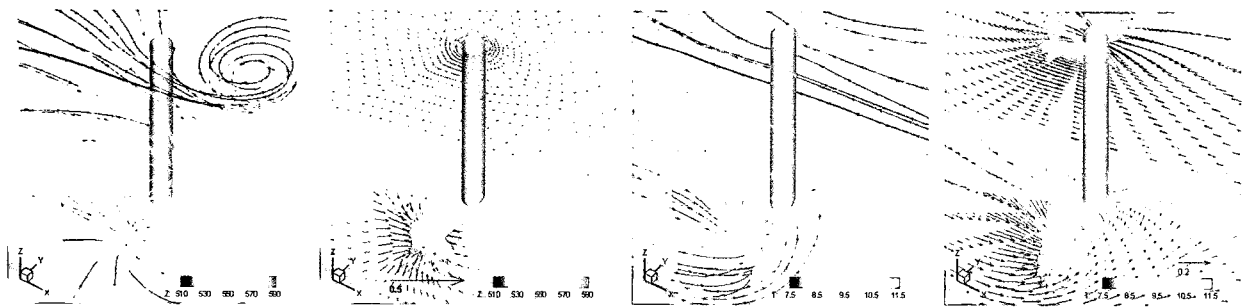


Fig. 7. Snapshots of instantaneous streamtraces and velocity vectors colored by elevation Fig. 8. Snapshots of instantaneous streamtraces and velocity vectors colored by temperature

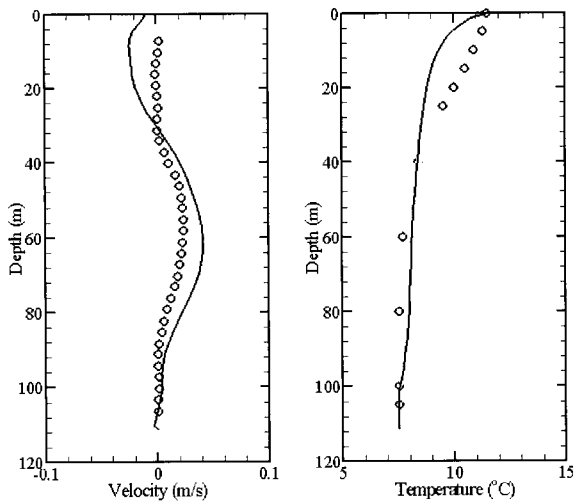


Fig. 9. Measured and computed velocity and temperature profiles in bottom withdrawal case: circle - measured; black line - computed, time-averaged; grey line - computed, instantaneous

## 5. Conclusions

A three-dimensional hydrodynamic model for simulating unsteady stratified flow in complex geometry has been developed. The evaluation results of the developed numerical model show that turbulent mixing of the temperature is enhanced as the Froude number increases and turbulence collapses for lower Froude numbers for which buoyancy effects dominate. The simple algebraic mixing length model employed in this study appears to perform very well as the Froude number is decreased but its performance deteriorates somewhat at higher Froude numbers.

The simulation results for the selective withdrawal in a geometrically complex reservoir show high unsteadiness of velocity field due to the thermal stratification even though the temperature profiles are relatively stable. The predictions of numerical simulation appear to capture the general shape of velocity and temperature profiles reasonably well, while significant overestimation of the magnitude of velocity profiles is observed. The present results demonstrate the need of extension of the computation domain further upstream taking account of reasonable inflow and temperature

profiles at the far-field boundary.

## References

- Debler, W.R. (1959). "Stratified flow into a line sink" *ASCE, J. Eng. Mech. Div.*, pp. 51-65.
- Fischer, H.B., List, E.J., Koh, R.C.Y., Imberger, J and Brooks, N.H. (1979). *Mixing in Inland and Coastal Water*. Academic Press, New York.
- Forbes, L.K. and Hocking, G.C. (2003). "On the computation of steady axi-symmetric withdrawal from a two-layer fluid." *Comput. Fluids*, Vol. 32, pp 385-401
- Imberger, J. (1972). "Two-dimensional sink flow of a stratified fluid contained in a duct." *Journal of Fluid Mechanics*, Vol. 53, pp. 329-349.
- Imberger, J. (1980). "Selective Withdrawal. A Review.", *Second International Symposium on Stratified Flows*, Trondheim, Norway, pp. 381-400.
- Ivey, G.N., and Blake, S. (1985). "Axisymmetric withdrawal and inflow in a density-stratified container." *Journal of Fluid Mechanics*, Vol. 161, pp. 115-137.
- Kundu, P.K. (1990). *Fluid Mechanics*, California: Academic Press.
- Mason, P.J. (1989). Large eddy simulation of the convective boundary layer." *J. Atmos. Sci.*, Vol. 45, pp. 1492-1516.
- Mason, P.J. and Thomson, D. J. (1992). "Stochastic backscatter in large-eddy simulation of boundary layers." *Journal of Fluid Mechanics*. Vol. 242, pp. 51-78.
- McGuirk, J.J. and Islam, S. A.K.M. (1987). "Numerical Modelling of the Influence of a Hood on Axisymmetric Withdrawal from a Density Stratified Environment." *Proceedings of the Third International Symposium on Stratified Flows*, Pasadena California, pp. 1047-1060.
- Paik, J., Sotiropoulos, F. and Sale, M. J. (2005). "Numerical simulation of swirling flow in a hydroturbine draft tube using unsteady statistical turbulence models." *Journal of hydraulic Engineering*, Vol. 131, No 6, pp. 441-456.
- Pao, H.-P. and Kao, T.W. (1974). "Dynamics of establishment of selective withdrawal of a

- stratified fluid from a line sink. Part 1. Theory." *Journal of Fluid Mechanics*, Vol. 65, part 4, pp. 657-688.
- Pao, H.-P., Kao, T.W., and Wei, S.N. (1974). "Dynamics of establishment of selective withdrawal of a stratified fluid from a line sink. Part 2. Experiment." *Journal of Fluid Mechanics*, Vol. 65, part 4, pp. 689-710.
- Poinsot, T.J., and Lele, S.K. (1992). "Boundary Conditions for Direct Simulations of Compressible Viscous Flows." *Journal of Computational Physics*, Vol. 101, pp. 104-129
- Rodi, W. (1987). "Examples of calculation methods for flow and mixing in stratified fluids." *Journal of Geophysical Research*, Vol. 92, No. C5, pp. 5305-5328.
- Sladkevich, M., Militeev, A.N., Rubin, H., and Kit, E. (2000). "Simulation of Transport Phenomena In Shallow Aquatic Environment." *Journal of Hydraulic Engineering*, Vol. 126, No.2, pp. 123-136.
- Sotiropoulos, F. and Abdallah (1992). "A Primitive Variable Method for the Solution of Three-Dimensional Incompressible Viscous Flows." *Journal of Computational Physics*, Vol. 103, pp. 336-349.
- Tang, H. S., Jones, S. C. and Sotiropoulos, F. (2003). "Domain Decomposition with overset grids for 3D incompressible flows." *Journal of Computational Physics*, Vol. 191, pp. 567-600.
- Thompson, K.W. (1990). "Time-Dependent Boundary Conditions for Hyperbolic Systems, II." *Journal of Computational Physics*, Vol. 89, pp. 439-461.
- Viollet, P.-L. (1980). "Turbulent Mixing in a Two-Layer Stratified Shear Flow." *Second International Symposium on Stratified Flows*, Trondheim, Norway, pp. 315-325.
- Wood, I.R. (2001). "Extensions to the theory of selective withdrawal." *Journal of Fluid Mechanics*, Vol. 448, pp.315-333.

(논문번호:05-02/접수:2005.01.08/심사완료:2005.10.05)